38/10-3-97 JSO(1)

# UNIVERSITY OF WISCONSIN

## CENTER FOR PLASMA THEORY AND COMPUTATION

# REPORT

**Required Conditions For And Coincident 1/1-Mode Activity Associated With The Nonlocal Electron Heat Transport Effect on TFTR**


*M. W. Kissick, J. D. Callen, E. D. Fredrickson*

Department of Nuclear Engineering & Engineering Physics
University of Wisconsin-Madison
Madison, Wisconsin 53706-1687



August 1997

**UW-CPTC 97-11**




MADISON, WISCONSIN 53706-1687

# Required Conditions For And Coincident 1/1-Mode Activity Associated With The Nonlocal Electron Heat Transport Effect On TFTR

M.W. KISSICK, J.D. CALLEN, E.D. FREDRICKSON*

*University of Wisconsin - Madison, 1500 Engineering Dr., Madison, WI 53706-1687, USA*

**Princeton Plasma Physics Lab., Princeton University, P.O. Box 451, Princeton, NJ 08543, USA*

ABSTRACT. A database of 71 distinct and randomly collected cold pulse cases from TFTR is analyzed. Observations show a striking parameter regime cutoff for the presence of nonlocal transient transport and coincident MHD (1/1-mode) activity as well as for changes in the radial speed of the nonlocal transport effect and changes in the sawtooth period. A nontrivial link is demonstrated between electron heat transport and MHD properties through observation of a common cutoff in the parameter $n_e(0)/T_e(0)^{1/2}$ and a common threshold in injection size for radial speed and sawtooth period changes. Auxiliary heating (via energetic neutral beams) destroys whatever process is responsible for the nonlocal transport effect, unless the discharge contains significant amounts of injected tritium. These observations are preliminary, but they represent important circumstantial evidence for mysterious propagation of changes in some MHD-related phenomenon as being responsible for a large fraction of electron heat transport. This propagation is then probably a function of $n_e(0)/T_e(0)^{1/2}$, ion mass, and possibly beam power. An analysis of Ohmic cases shows that the cutoff in $n_e(0)/T_e(0)^{1/2}$ indicates the nonlocal transport effects may occur when the electrons are collisionally thermally decoupled from the ions.

## I. Introduction

The initial transient transport studies [1,2] were intended to simply complement the usual power balance methods which determine the electron heat diffusion coefficient in tokamaks. However, the transient values of this diffusivity were found to be quite different from the power balance values, and this difference was shown to be quite complex [3-8]. The initial cold pulse propagation study [9] was also intended to complement the previous transient methods (mostly sawtooth heat pulse propagation). However, in like fashion, it too was shown to be quite complex [10,11,12] by having a very noticeable nonlocal aspect to the transport behavior. Here, "nonlocal" refers to the situation where the transport coefficients cannot be wholly described by functions and combinations of spatially local variables. In other words, there was shown to be a component of the transient transport behavior that could not be described by a single parabolic partial differential equation (even nonlinear) with coefficients all functions of position (explicit or implicit). This nonlocal effect was manifested by a mysterious rise in the central electron temperature, $T_e$, induced by rapid edge cooling (see Figures 1 and 2 for a view of this effect: both are from reference [12]). This rise happened so quickly and with such a large magnitude that it could not be explained by the impurities which caused the edge cooling, nor the redistribution of current or flux surfaces. This central $T_e$ rise was simply not a relaxation process; therefore, it must be related to a traveling change in whatever causes the anomalous transport.

The $T_e$ rise (see Figures 1 and 2) was not observed at first (see Figure 3) and only appears in certain situations. This paper presents an attempt to understand the

parametric dependencies of this nonlocal effect and other, concomitant MHD (Magnetohydrodynamic) effects (e.g., changes in $m/n = 1/1$ mode activity and sawteeth). The reader is encouraged to read references [9,10,12] for a review of how cold pulse propagation studies lead to observations of nonlocal transport.

In this paper, we present results from looking at a fairly large number (71) of randomly collected cold pulse cases from TFTR [13]. Most of the cases that make up this database are random carbon flakes from the TFTR vessel wall which have previously been shown [11] to act like (generally large) laser-ablation impurity injections in cold pulse and nonlocal effect studies. In addition, some pellets are small and/or slow enough to produce a similarly small perturbation of localized (to the outer plasma) cooling before they ablate. Results from this database as well as a careful look at a previously studied case [11,12] provide a great deal of new information which is presented now in this paper. Since this work is ongoing, the purpose of this paper is to quickly present new observations with only hints towards possible implications for theory.

## II. The Database

The database includes three types of sources for the cold pulses (edge cooling induced temperature perturbation): laser-ablation injection of impurities [14], random carbon flakes from the TFTR vessel wall, and pellet injection (smaller or slower pellets). So far we have found 85 distinct recorded cold pulse cases. Some of the injection cases represent ensembles of similar injections in similar discharges. Of the 85 cases, there are 3 shots that contain significant tritium, 28 Ohmic shots, and 43 beam heated shots. However, for 14 shots, some of the data is still too incomplete to use. All of these cases were stumbled upon by looking at data from old shots. Thus, they represent a random sampling of TFTR plasma conditions. The ranges of some key parameters are as follows: 0 MW < $P_{beam}$ < 32 MW, $0.7X10^{19}$ $m^{-3}$ < $n_e(0)$ < $7X10^{19}$ $m^{-3}$, 0.8 keV < $T_e(0)$ < 9 keV, 0.98 MA < $I_p$ < 2.52 MA. The time during the discharge of the cold pulse ranges from 0.5 s to 5.3 s. The shot numbers range from 31880 to 93659. We suspect that these cases represent a minuscule fraction of the total cold pulse cases for all TFTR discharges.

Many quantities were examined including plasma current and toroidal magnetic field, but the electron density, and to some extent, electron temperature were the only quantities found so far that show a correlation to the presence or absence of nonlocal transport behavior (besides tritium content and beam power which are discussed below). The central electron density is determined from Abel inversions of data from a 10-channel far-infrared interferometer [15]. The electron temperature was measured by both a 20-channel ECE (electron cyclotron emission) grating polychromator [16] for the time behavior at various radii, and also by the ECE Michelson interferometer [17] for the magnitude of the central electron temperature. The polychromator data has excellent temporal and spatial resolution but its data need magnitude calibration from the Michelson interferometer data.

Of the 71 cases which seem to have a reasonable amount of good and complete data, 20 show a nonlocal transport effect to a large enough degree that it is unambiguous to the eye upon examining the polychromator data. The nonlocal transport effect is manifest in the data by a transient core electron temperature, $T_e$, rise due to the rapid cooling at the edge. Previous years of work have demonstrated that this type of core $T_e$ rise is due to a drop in the core electron heat transport ahead of changes in local core quantities [10-12]. The term "nonlocal" in this sense is relative to local plasma parameters and transport. That is, we presume some local propagation related to the cause of anomalous transport itself must have occurred. It is hoped that the following observations will help shed light on the nature of this propagation of some change in the transport and therefore the nature of what causes the transport itself.

## II.a Ohmic cases

The clearest observations come from the Ohmic cases. Cases with beam heating are roughly consistent, but the Ohmic cases are more straightforward as will be discussed in the next section. The most significant parameters that seem to determine whether the nonlocal transport effect happens or not are electron density and, to a lesser extent, temperature: specifically, electron density relative to a weaker function of electron temperature. A rough way to present this dependence is to make a histogram of these cases versus the central electron density, $n_e(0)$, divided by the square root of the central electron temperature, $T_e(0)$ (see Figure 4b). In Figure 4b, the above described histogram is shown, and we notice that there is a distinct cutoff at around $n_e(0)/T_e(0)^{1/2} \sim 0.035 \times 10^{19}\ m^{-3}/eV^{1/2}$. Above that cutoff we observe an ordinary cold pulse propagating diffusively inward from the edge with no core $T_e$ rise. This cutoff is also delineated by borderline cases which show only a slight hint of a nonlocal rise in the core $T_e$. In addition to Figures 1 and 2 (shot 31889), see Figure 5 for another example of a strong nonlocal effect in an Ohmic discharge.

The quantity $n_e(0)/T_e(0)^{1/2}$ used above may be a very rough approximation to a more exact expression. The same picture presents itself for $n_e(0)/T_e(0)$ (see

Figure 4a) and also $n_e(0)/T_e(0)^{3/2}$ (see Figure 12 in section IV.c). Nonetheless, $n_e(0)/T_e(0)^{1/2}$ seems to work best (it separates the groups further in the histogram: see Figure 4b versus 4a). The use of $n_e(r=0)$ and $T_e(r=0)$ may be less relevant than some sort of global measure of $n_e$ and $T_e$, or perhaps $n_e(r=r_{mix})$ and $T_e(r=r_{mix})$ , where $r_{mix}$ is the sawtooth mixing radius, is best. It is possible that a variety of exponents, m, in $n_e(0)/T_e(0)^m$ may also work. A value of m = 0 does not work well (see Figure 4c) as will be discussed later in section IV.b. If m = 1 is used, the beam heated cases are inconsistent with the Ohmic cases. We therefore choose to use $n_e(0)/T_e(0)^{1/2}$ for the discussion and presentation of these general observations.

## II.b Beam heated cases and tritium influence

For the beam heated cases, we do not observe any nonlocal transport effect -- UNLESS there is tritium in the plasma. Of the 43 beam heated cases, only 3 show a noticeable $T_e$ rise due to the cold pulse, and all 3 cases are tritium shots (Figure 7 of [12] presents one such tritium case). We presume this tritium dependence translates into an ion mass dependence of the nonlocal effect. The effect of beam heating may be to simply increase $n_e(0)/T_e(0)^{1/2}$ [mainly through an increase in $n_e(0)$ with increasing beam power]. In Figure 6, we notice that the beam heated cases all fall above the cutoff in $n_e(0)/T_e(0)^{1/2}$, with the exception of just one case. Other studies with radio frequency heating have indicated that auxiliary power reduces the nonlocal effect [10], or has no affect [18]. We wish there were more beam heated cases in this database that show the nonlocal effect (beyond the three tritium cases) in order to better determine the beam's effects. However, at this point, the beam heated cases seem roughly consistent with the cutoff in

$n_e(0)/T_e(0)^{1/2}$ with the exception of the tritium dependence which is still mysterious.

## II.c Relation to MHD behavior

Related to the above nonlocal transport observation are observations of apparent nonlocal interactions with MHD (1/1 mode) activity. It was previously observed [11,12] that the sawtooth period underwent a transient period increase or decrease COINCIDENT in time with the nonlocal $T_e$ rise (see Figures 1 and 5). In addition to the temporal coincidence, the nonlocal MHD behavior is roughly coincident with the cutoff in $n_e(0)/T_e(0)^{1/2}$ described above for the nonlocal transport behavior (see Figure 7). In the higher $n_e(0)/T_e(0)^{1/2}$ cases, fishbones, and other 1/1-mode MHD activities are sometimes instantaneously triggered by the edge cold pulse, but ahead of the diffusive propagation of the cold pulse into the core or without significant local parameter changes in the core (see Figure 8). The sawtooth period tends to increase transiently when there is a $T_e$ rise (nonlocal transport effect), and transiently decrease without the $T_e$ rise. The only exception to this sawtooth trend is the case of the ensemble 31880-31891 (analyzed in a previous paper [12]). This exception case has a relatively high $n_e(0)/T_e(0)^{1/2} \sim 0.029 \times 10^{19}\ m^{-3}/eV^{1/2}$ for a case that shows a $T_e$ rise and is near the cutoff. In Figure 7, this exception case is the borderline case with a low $n_e(0)/T_e(0)^{1/2}$. From this ensemble, we learn that the injection size is an important factor in agreement with [10]. See section III for more discussion of this ensemble (the sawtooth period near the cutoff can either increase or decrease depending on the size of the injection).

In Figure 7, the same type of histogram is presented as in Figure 4. The cutoff is basically identical to one presented in Figure 4b. Here, we observe that both the sawtooth period decrease and the triggering of other MHD (1/1 mode) activity is correlated somehow with the absence of the nonlocal transport effect. The nonlocal transport effect then seems related to the transient stablization of MHD (an increase of the sawtooth period is like a stabilization of the 1/1 precursor). Previously, we have interpreted this coincidence with MHD transients to hint at a role for electromagnetics in electron heat transport [11,12].

### III. The 31880-31891 ensemble

This ensemble was previously analyzed to a great extent [11,12], and was originally performed to explore trace impurity transport [19]. Left out of that previous analysis and discussion were observations of slight differences from one shot and injection to the other. There is much valuable information in these differences, because this ensemble sits close to the above described cutoff in $n_e(0)/T_e(0)^{1/2}$. There are laser-ablation injections of aluminum in shots 31880,31881,31885-31891 at varying magnitudes. The size of the injection is measured by the relative change in radiation, or equivalently for a temporally sharp injection, the relative change in the magnetically measured plasma surface loop voltage.

There are two related and striking observations in this ensemble. First, the transient and nonlocal relative sawtooth period change that is coincident with the nonlocal transport effect (core $T_e$ rise) is constant and negative for smaller injections (relative loop voltage perturbation less than 0.7, see Figure 9). Also, in Figure 9, one can observe a striking threshold where the relative sawtooth period perturbation increases for larger injections and becomes positive (relative loop voltage perturbation greater than 0.7). The second observation made from this same ensemble involves the speed of the $T_e$ rise (nonlocal transport effect). In Figure 10, one can notice that the time of the peak of the core $T_e$ rise increases (propagation speed of some transport change decreases) as the injection size increases UNTIL the same point (0.7) of relative loop voltage perturbation is reached. The $T_e$ rise timing between r = 0.28 m and r = 0.10 m above that point in injection size is consistent with what we expect a propagation of a transport change diffusing at the local power balance electron heat diffusion rate to be, as follows. If one assumes a slab approximation between these nearby radii (r = 0.28 m and r = 0.10 m) and takes a partial time derivative of a Gauss Kernel for the diffusion propagator [20] and set it equal to zero to get the "time-to-peak," $t_p$, then one obtains $\Delta t_p = 0.5\ (\Delta r)^2/\chi_e$, where $\chi_e$ is the electron heat diffusivity. If we use $\Delta r = 0.18$ m, and $\chi_e = 0.5\ m^2/s$ from the transport code SNAP for this ensemble, then $\Delta t_p = 0.032$ s which is very close to 0.065 s - 0.035 s = 0.030 s from Figure 10 for the difference in $t_p$ of the 31891 points.

Therefore, there is a coincidence in threshold behavior between the nonlocal transport effect speed and the nonlocal sawtooth change behavior. For this ensemble, there appears to be a physical process that can only be accessed at a large enough injection size. This coincident behavior between speed and sawtooth change can be seen in Figure 11 where the central ECE channels for four of the shots in the ensemble are shown. Because the Te rise lasts longer for larger injections (a time more comparable to equilibrium transport time scales), this threshold may possibly be a reflection of when the local electron density gradient perturbation near the, safety factor, q = 1 surface starts to become important to the sawtooth dynamics. Many of the carbon flakes are large enough to induce a significant electron density perturbation (mostly at a later time). However, the aluminum laser-injections presented here are very small: $\Delta n_e < 1$ % for $r/a < 0.5$ for all time [12]. The bigger mystery may be the apparent triggering of 1/1 mode activity for the higher $n_e(0)/T_e(0)^{1/2}$ cases (see Figure 8) that seems to respond instantly to modulations in the plasma loop voltage measured by magnetics at the plasma edge [11].

## IV. Discussion

We feel that the importance of the above observations cannot be emphasized enough. Perhaps, for the first time, there is some hope in getting a clearer picture of electron heat transport. Both the observations related to $n_e(0)/T_e(0)^{1/2}$ (and the role of tritium and beam power) as well as the sawtooth and radial speed observations from the 31880-31891 ensemble are remarkable in themselves, but taken together, a powerful picture begins to emerge of electron heat transport intimately coupled with MHD-related phenomena.

### IV.a The 31880-31891 ensemble

From the 31880-31891 ensemble, we notice two distinct physical effects: a smaller injection accesses the physical effect of enhanced propagation behavior for the $T_e$ rise (which is related to sawtooth destablization and the triggering of 1/1 modes), but a larger injection displays an entirely different phenomenon. Larger injections slow the maximum in the $T_e$ rise to a speed consistent with the power balance value of the electron heat diffusion (and this seems related to sawtooth stablization). It almost seems as if the power balance electron heat transport could be reflecting a lower limit of how slow changes can transport, and this phenomenon is related to the nonlocal transient sawtooth stablization. There is a clear connection between MHD (1/1 mode) activity and transport here. However, this connection is not necessarily causal. Since the nonlocal transport effect (core $T_e$ rise) happens for all the injections in the 31880-31891 ensemble (basically proportional to the injection size), one might say that the sawtooth (MHD) transient and the nonlocal effect have the same cause, but do not cause each other. This same cause is likely the propagating change in some unknown quantity initiated at the plasma edge by the cold pulse.

### IV.b Histograms and the role of density

From the $n_e(0)/T_e(0)^{1/2}$ histogram observations in the database, we again notice two distinct physical effects. Below the cutoff [$n_e(0)/T_e(0)^{1/2} \sim 0.035 \times 10^{19}$ m$^{-3}$/eV$^{1/2}$], one can observe a nonlocal transport effect from the cold pulse in Ohmic cases, and this effect is correlated with a sawtooth period increase just as is the case with the 31880-31891 ensemble when the injection size is large enough (see Figure 9). Above this cutoff, there is simply the enhanced cold pulse propagation in Ohmic cases (like the original case [9], see Figure 3), but there is also a tendency to trigger or destablize MHD behavior (1/1 modes) as evidenced by nonlocally and transiently decreasing the sawtooth period. The 31880-31891 ensemble sits on the boundary (near the $n_e(0)/T_e(0)^{1/2}$ cutoff) where we see the nonlocal transport effect, but we see a varying nonlocal MHD effect. Beams seem to destroy the nonlocal transport effect, and tritium seems to enhance it. However, the beam heated cases seem roughly consistent with the $n_e(0)/T_e(0)^{1/2}$ cutoff. They are not consistent with the independent variable $n_e(0)/T_e(0)$ which we had originally suggested [21].

The role of density in the above mentioned histograms seems more important than the role of temperature, but a weaker temperature dependence is still required. In Figure 4a, we plot the Ohmic cases just versus density: the groups do not separate well partly due to two low density cases that do not show a $T_e$ rise, and both of these cases have very low temperatures. Other research [10,18] indicates only the density dependence, but they do not have the wide variety of conditions present in this study. Perhaps this density dependence is somehow related to the observation that the "ballistic effect" [4,5] in sawtooth heat pulse propagation is stronger for lower densities [4]. In addition, we know that a low $n_e(0)/T_e(0)^{1/2}$ is similar to a low electron-ion collision frequency, so the nonlocal transport effect may be related to more collisionless conditions. Perhaps $Q_{ei}$ (the electron-ion heat transfer rate from collisions) is important since it scales as the electron-ion collision frequency times the plasma pressure ($n_eT_e$) which yields $n_in_e/T_e^{1/2}$. In any case, the nonlocal effect happens in the low collisionality range where we expect weaker electron-ion heat coupling which means it is really caused more by the electron channel and not the coupling with the ion channel. With the observations of transport changes due to the new enhanced reversed shear mode, the electron and ion heat transport channels do appear to be quite different since the electron heat transport channel is only slightly affected by the reversed magnetic shear (versus the ion heat transport channel in which the transport becomes neoclassical)!

### IV.c A collisional coupling cutoff for nonlocal effects

There is reason to think that the $n_e(0)/T_e(0)^{1/2}$ cutoff for nonlocal transport is possibly related to electron-ion collisionality, as mentioned above. Consider just the Ohmic cases (where all species are basically in a Maxwellian energy distribution) and assume a simple two-species energy conservation equation,

$$\frac{3}{2} n_e \frac{dT_e}{dt} = -3\left(\frac{m_e}{m_i}\right)\frac{n_e}{\tau_e}\left(T_e - T_i\right), \tag{1}$$

where, $m_e$, $m_i$, $n_e$, $T_e$, and $T_i$ are the electron mass, ion mass, electron density, electron temperature, and ion temperature respectively. We have implicitly included the divergence of the heat flux in the total time derivative. The quantity, $\tau_e$, is the energy transfer time between assumed Maxwellian distributions,

$$\tau_e \approx \left(3.4X10^{11} s\right)\left(\frac{1}{\ln \Lambda}\right)\left(\frac{T_e^{3/2}}{n_e}\right), \tag{2}$$

where, $\ln \Lambda$ is the Coulomb Logarithm. The quantity, $T_e$, is measured in eV and $n_e$ is measured in standard SI units ($m^{-3}$). We can also define an energy equilibration time between the two species,

$$\tau_\infty \equiv \left(\frac{m_i}{m_e}\right)\frac{\tau_e}{4} z^{-3/2}, \tag{3}$$

where $z \equiv T_e / T_\infty$ and $T_\infty \equiv (T_e + T_i)/2$. A third time scale is the electron energy confinement time, $\tau_{Ee}$, which is a measure of how fast heat is transported spatially within the electron channel. A quantity which measures the relative thermal isolation of the electron heat channel is the ratio of the above time scales, R:

$$R \equiv \frac{\tau_{Ee}}{\tau_{\infty}}, \tag{4}$$

which is $Q_{ei} / \nabla \bullet q_e$ for steady-state with $Q_{ei}$ = energy transfer rate between electrons and ions, and $q_e$ = electron heat flux. We can get an order of magnitude estimate for R by assuming no spatial dependencies in $\tau_e$, and a constant $\tau_{Ee}$= 0.1 s with no spatial dependencies. Then, to within an order of magnitude at about the half radius for typical Ohmic plasmas,

$$R \approx \frac{\tau_{Ee}}{\tau_e}\left(\frac{m_e}{m_i}\right)6$$

or

$$R \approx \left(3.2X10^{-14}\right)\left(\frac{n_e(0)}{T_e(0)^{3/2}}\right). \tag{5}$$

The observed cutoff, $n_e(0)/T_e(0)^{1/2} \sim 0.035 \times 10^{19}\ m^{-3}/eV^{1/2}$ is then equivalent to $3 < R < 5$ if we put the database values into Eq. (5) (see Figure 12). The interesting point is that for <u>Ohmic cases</u>, the cutoff estimate for nonlocal transport is $1 < R < 10$. Therefore, we observe the nonlocal transport effect for Ohmic cases when the electrons are mostly collisionally thermally decoupled from the ions.

However, at this stage, the beam heated cases seem inconsistent with this picture of collisional decoupling if $R \sim n_e(0)/T_e(0)^{3/2}$: they would be consistent if $R \sim n_e(0)/T_e(0)^{1/2}$. It should be noted again though, we need more beam heated cases with a $T_e$ rise in order to make firmer statements regarding auxiliary heating (such as the effects of nonMaxwellian ions, etc.) An excellent experiment would be to acquire more auxiliary heating cases, albeit on another machine since TFTR is decommissioned. The beneficial effects of tritium are also a mystery, but the qualitative trend of R with increased ion mass is consistent [see Eqs. (3) and (5)]. Future work will be concerned with understanding the roles of auxiliary heating and isotopes.

### IV.d Towards a better picture of electron heat transport

The next interesting step is to attempt to expand the observations from the 31880-31891 ensemble to other cases in the database. Work along these lines has only begun, and it is made difficult by the fact that in most of the other cases in the database, there is only one random flake (generally equivalent to a sizable laser-ablation injection) rather than an ensemble of controlled impurity injections as in the 31880-31891 ensemble. In general though, the phenomenon associated with the larger injections of the 31880-31891 ensemble seems more enhanced for lower $n_e(0)/T_e(0)^{1/2}$ Ohmic cases. It is likely that the injection magnitude threshold of 0.7 for the relative loop voltage perturbation in the 31880-31891 ensemble is a function of density relative to the square root of temperature. Perhaps, the lower $n_e(0)/T_e(0)^{1/2}$ is, the lower this threshold is.

All of the above observations point to a different picture of the turbulence in tokamaks. There appears to be some form of rapid radial propagation in whatever is responsible for anomalous electron heat transport. We know that the core $T_e$ rise from the impurity injection is a nonlocal transport effect [10-12], and there appears to be propagation of something causing the rise (see Figures 1, 5, and 10). However, because the magnitude of the $T_e$ rise is larger further in (see Figure 2), it cannot be a relaxation process in electron temperature. Therefore, the propagation must be a propagation in something causing the electron heat transport -- presumably plasma turbulence. There are various theories which describe various forms of turbulence propagation [22-24]; however, it is still very unclear how to fit the theories into the picture presented by this data.

In addition to the propagation of some change in whatever causes anomalous electron heat transport, these observations also very strongly point to an interesting interaction with magnetics (in the form of coincident transients in MHD (1/1 mode) activity with corresponding threshold behaviors). Recent observations from the RTP tokamak demonstrate very nontrival and significant transport interactions with low mode number MHD behavior [25]. There are also new turbulence theories which point to lower mode number MHD-type behavior [26].

## V. Conclusions

New observations from both a database of random cold pulse cases and differences within a previously analyzed ensemble of laser-ablation injection cold pulses point towards several trends of nonlocal electron heat transport and MHD activity (1/1 modes and changes in sawteeth) . A cutoff in $n_e(0)/T_e(0)^{1/2}$ is observed for the onset of nonlocal transport behavior (core $T_e$ rise) induced from rapid edge cooling (cold pulses). This nonlocal transport cutoff is similar to the cutoff observed for nonlocal MHD activity changes. That is, below approximately the same cutoff value of $n_e(0)/T_e(0)^{1/2} \sim 0.035 \times 10^{19}\ m^{-3}/eV^{1/2}$, the sawteeth tend to transiently increase their period coincident with the nonlocal $T_e$ rise. Above that cutoff, there is a transient decrease in the sawtooth period, and in some cases, other MHD phenomena (1/1, fishbones) seem to be triggered from a distance. The nonlocal transport effect seems to correlate with, but not necessarily to be causally linked to, a nonlocal MHD activity stablization. This cutoff in $n_e(0)/T_e(0)^{1/2}$ is likely related to the significance of the Coulomb-collision-induced thermal coupling. That is, based on the Ohmic cases alone, we see the nonlocal electron heat transport effect when the electrons are collisionally thermally decoupled from the plasma ions. A role for $T_e(0)$ in the above observations is required, but more work is required to determine the exact dependence. Density is a more important variable.

From differences related to the size of the impurity injection in the 31880-31891 ensemble from one shot to another, the link between MHD activity and electron heat transport is further strengthened. As the injection size increases, the time required for the $T_e$ rise to reach its maximum increases. This "time-to-peak" for the $T_e$ rise levels off at a value coincident with the local power balance electron heat diffusivity value at the same injection size that marks the threshold from transient sawtooth destablization to stablization.

The general picture that emerges is that electron heat transport is related to propagating changes in the character of whatever is responsible for its anomalous transport. This mysterious propagation seems to affect: 1) MHD stability (of 1/1 modes and sawteeth), 2) seems to have a cutoff behavior in electron density relative to the square root of electron temperature that may indicate a purely electron behavior, 3) and seems to also be sensitive to ion mass and possibly auxiliary power. The propagation, which causes the $T_e$ rise, seems to travel faster for smaller perturbations, but it travels no slower than diffusion at the power balance value of the effective electron heat diffusivity. The power balance value of the electron heat diffusivity is possibly a reflection of this threshold behavior in some physical process of propagating changes. The transient values of the electron heat diffusivity, which have always appeared different from the power balance values, may be complicated by transients in the possible plasma turbulence itself, though likely in a nontrivial manner.

## Acknowledgments:

The authors gratefully acknowledge very useful conversations with X. Garbet, R. Sydora, and C. Hegna. A great deal of appreciation is also extended to the entire TFTR physics and technical staff. This work was supported by U.S. Department of Energy Grant DE-FG02-92ER54139 and TFTR through U.S. Department of Energy contract DE-AC02-76-CHO-3073.

## References:

[1] CALLEN, J.D., and JAHNS, G.L., Phys. Rev. Lett. **38** (1977) 491.

[2] SOLER, M., and CALLEN, J.D., Nucl. Fusion **19** (1979) 703.

[3] FREDRICKSON, E.D., et al., Nucl. Fusion **26** (1986) 849.

[4] FREDRICKSON, E.D., et al., Phys. Rev. Lett. **65** (1990) 2869.

[5] FREDRICKSON, E.D., et al., Nucl. Fusion **33** (1993) 1759.

[6] JACCHIA, A., et al., in Controlled Fusion and Plasma Physics, (Proc. 22nd EPS conf., 3-7 July, 1995, Bournemouth, UK), Vol. 19C, Pt. 3, EPS, UK (1995) 9.

[7] PARAIL, V.V., et al., Nucl. Fusion **37** (1997) 481.

[8] CORDEY, J.G., et al., Nucl. Fusion **35** (1995) 101.

[9] KISSICK, M.W., et al., Nucl. Fusion **34** (1994) 349.

[10] GENTLE, K.W., et al., Phys. Plasmas **2** (1995) 2292.

[11] KISSICK, M.W., et al., Bull. Am. Phys. Soc. **39** (1994) 1678.

[12] KISSICK, M.W., et al., Nucl. Fusion **36** (1996) 1691; Nucl. Fusion **37** (1997) 568.

[13] HAWRYLUK, R.J., et al., in Plasma Physics and Controlled Nuclear Fusion Research 1986 (Proc. 11th Int. Conf. Kyoto, 1986), Vol. 1 IAEA, Vienna (1987) 51.

[14] MARMAR, E.S., et al., Rev. Sci. Instrum. **46** (1975) 1149.

[15] MANSFIELD, D.K., et al., Applied Optics **26** (1987) 4469.

[16] CAVALLO, A., et al., Rev. Sci. Instrum. **59** (1988) 889.

[17] STAUFFER, F.J., et al., Rev. Sci. Instrum. **56** (1985) 925.

[18] MANTICA, P., et al., "Non-local Plasma Response Induced By Peripheral Perturbations In The RTP Tokamak," in Controlled Fusion and Plasma Physics, (Proc. 24th EPS conf., 9-13 June, 1997, Berchtesgaden, Germany), post-deadline paper to be published in the proceedings.

[19] STRATTON, B.C., et al., Nuc. Fusion **29** (1989) 437.

[20] STAKGOLD, I., Green's Functions And Boundary Value Problems, Wiley, New York, 1979.

[21] CALLEN, J.D. and KISSICK, M.W., "Evidence And Concepts For Nonlocal Transport", in Controlled Fusion and Plasma Physics, (Proc. 24th EPS conf., 9-13 June, 1997, Berchtesgaden, Germany), invited paper T104 to be published in Plasma Physics and Controlled Fusion.

[22] GARBET, X., et al., Nuc. Fusion **34** (1994) 963.

[23] GARBET, X. and WALTZ, R.E., Phys. Plasmas **3** (1996) 1898.

[24] DIAMOND, P.H. and HAHM, T.S., Phys. of Plasmas **2** (1995) 3640.

[25] LOPEZ CARDOZO, N.J., et al., "Electron Thermal Transport In RTP: Filaments, Barriers And Bifucations," in Controlled Fusion and Plasma Physics, (Proc. 24th EPS conf., 9-13 June, 1997, Berchtesgaden, Germany), invited paper TL14 to be published in Plasma Physics and Controlled Fusion.

[26] CALLEN, J.D., and HEGNA, C.C., Bull. Am. Phys. Soc. **40** (1995) 1875.

**Figure Captions:**

Figure 1. Autoscaled ECE signals of the electron temperature in TFTR shot 31889 from the low field side. Note that the cold pulse starting from the edge mysteriously changes sign near minor radius, r = 0.28 m. See references [11,12] for more analysis of this example of the nonlocal transport effect. This member of the 31880-31891 ensemble was shown to be consistent with nonlocal electron heat transport observations on TEXT [10].

Figure 2. Averaged maximum electron temperature perturbation magnitudes for the ensemble of injections in shots 31880-31891. Note that the central electron temperature rise is larger nearer the core: it is not a heat pulse from the edge.

Figure 3. Autoscaled ECE signals of the electron temperature in TFTR shot 49971 from the low field side. The cold pulse starting from the edge was observed to propagate four times faster than the power balance prediction in the region $0.38 < r/a < 0.56$. See reference [9] for more details. This is an example of a case where no significant nonlocal effect has occurred, and this L-mode is powered by 12.5 MW of beam power.

Figure 4. Histogram of Ohmically heated TFTR cases which displays the cutoff in whether the nonlocal transport effect (core $T_e$ rise) occurs. (a) The cutoff occurs in $n_e(0)/T_e(0)$ (central electron density relative to central electron temperature). (b) The cutoff is more defined in the quantity $n_e(0)/T_e(0)^{1/2}$. (c) With just $n_e(0)$ alone, the groups do not separate well. Therefore, some $T_e(0)$ dependence seems necessary. See text for further discussion.

Figure 5. Autoscaled ECE signals of the electron temperature for TFTR shot 89168 from the low field side. This case is an example of a typical Ohmically heated nonlocal transport observation. Note that the central $T_e$ rise seems to be initiated near the edge and propagates inward, but just as with the 31880-31891 ensemble (see Figures 1,2), the magnitudes of the rise are larger further in. Note also that the sawtooth period change is coincident with the rise. Here, the variable R is the major radius.

Figure 6. Histogram for both the Ohmic cases of Figure 4 and neutral beam heated cases which displays the fact that the beam heated cases are roughly consistent with the Ohmic cases of Figure 4b. Also note that beams nullify the nonlocal transport effect, EXCEPT if there is significant tritium present. There is only one case out of 71 total that violates the cutoff at about $n_e(0)/T_e(0)^{1/2} \sim 0.035 \, X10^{19} \, m^{-3}/eV^{1/2}$ (with the interesting exception of the three tritium cases).

Figure 7. Histogram of all cases where a nonlocal transient triggering or modification of MHD (m/n = 1/1 mode activity) or sawtooth behavior is observed coincident with the cold pulse. These cases include both Ohmic and beam heated shots. If a decrease in the sawtooth period is caused by enhanced 1/1 instability, then there is a cutoff similar to Figure 4b in whether MHD activity is more stabilized or more destablized.

Figure 8. Autoscaled ECE signals of electron temperature from TFTR shot 89227 from the low field side which show the apparent triggering of a 1/1 mode by a carbon flake in a beam heated case. Note that the nonlocal transport effect (core $T_e$ rise) does not seem to be present; rather, here there is simply a (nonlinear) cold pulse diffusively propagating inward from the edge as in Figure 3.

Figure 9. From the 31880-31891 ensemble of laser-ablation injections of aluminum, the relative sawtooth period perturbation displays a sharp threshold behavior. This threshold occurs at an injection and cold pulse magnitude that causes a relative loop voltage perturbation of about 0.65. The relative loop voltage perturbation is proportional to the relative radiative power perturbation at the edge which in turn is proportional to the injection size. It is interesting that the relative sawtooth perturbation is positive above an injection size corresponding to a relative loop voltage perturbation of 0.7.

Figure 10. From the 31880-31891 ensemble of laser-ablation injection of aluminum, the "time-to-peak" or time of the maximum in the $T_e$ rise for two radii is plotted against the relative loop voltage perturbation (proportional to the injection size). Note that at a relative loop voltage perturbation of 0.7, the speed of whatever causes the $T_e$ rise levels off. The speed at which it levels off is consistent with the power balance electron heat diffusion rate between these radii. Note that the leveling off threshold occurs at the same relative voltage magnitude as for sawtooth changes in Figure 9.

Figure 11. Autoscaled ECE signals of electron temperature from four shots of the 31880-31891 ensemble of the central (r = 0.02 m) channel. The behavior indicated in Figures 9 and 10 is clearly noticeable. The magnitudes of the $T_e$ rise are basically proportional to the size of the injection -- no threshold in $T_e$ rise magnitude is noticeable.

Figure 12. Histogram of the same Ohmically heated cases as in Figure 4. Here they are plotted versus the R factor which is defined in Eqs. (4) and (5). Note that the cutoff for the nonlocal effect is between 1 and 10 which is what one would expect if the cutoff is related to a significance of electron-ion collisional thermal coupling.

FIG. 1

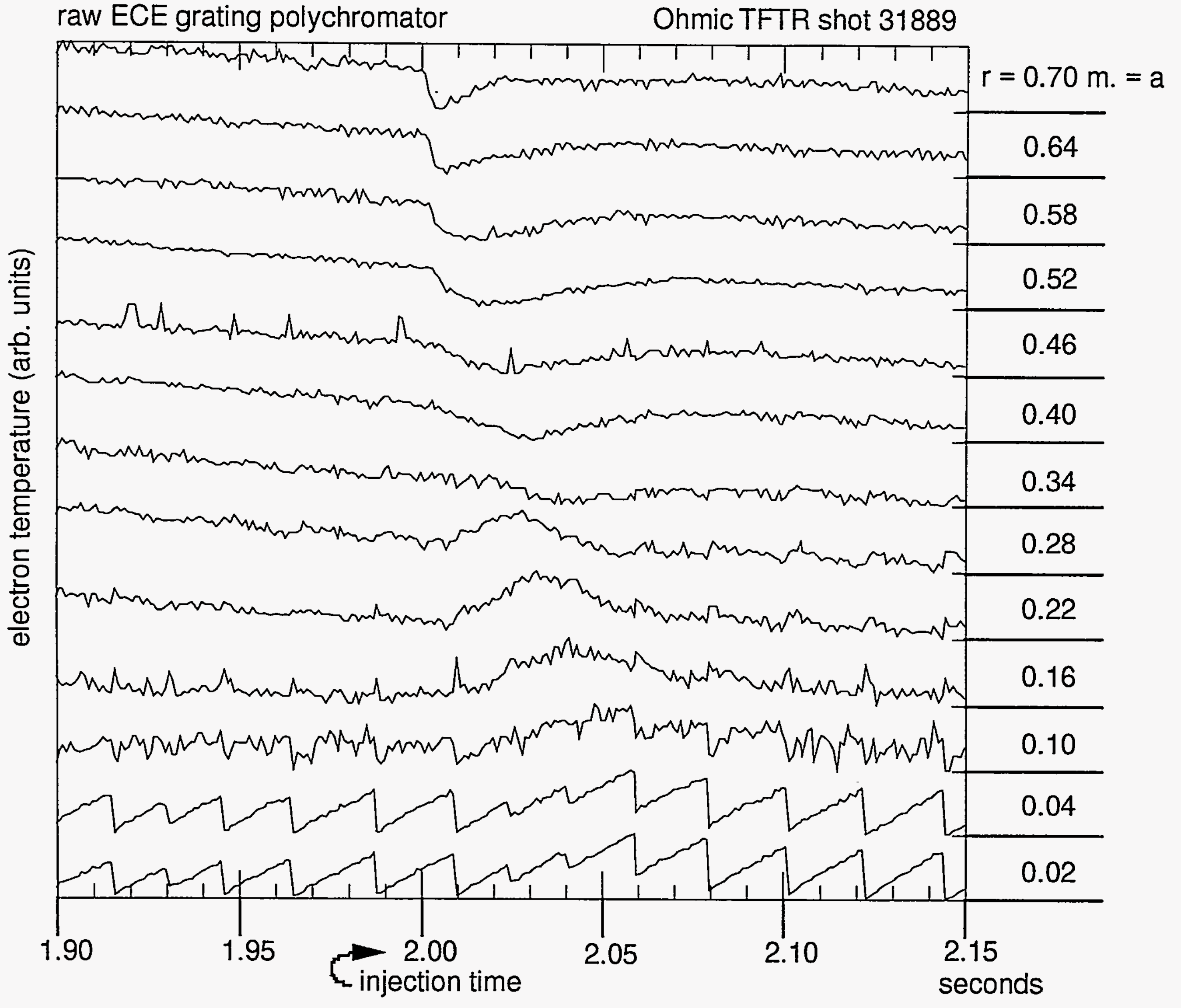
raw ECE grating polychromator
Ohmic TFTR shot 31889
electron temperature (arb. units)
r = 0.70 m. = a
0.64
0.58
0.52
0.46
0.40
0.34
0.28
0.22
0.16
0.10
0.04
0.02
1.90
1.95
2.00
2.05
2.10
2.15
injection time
seconds

FIG. 2

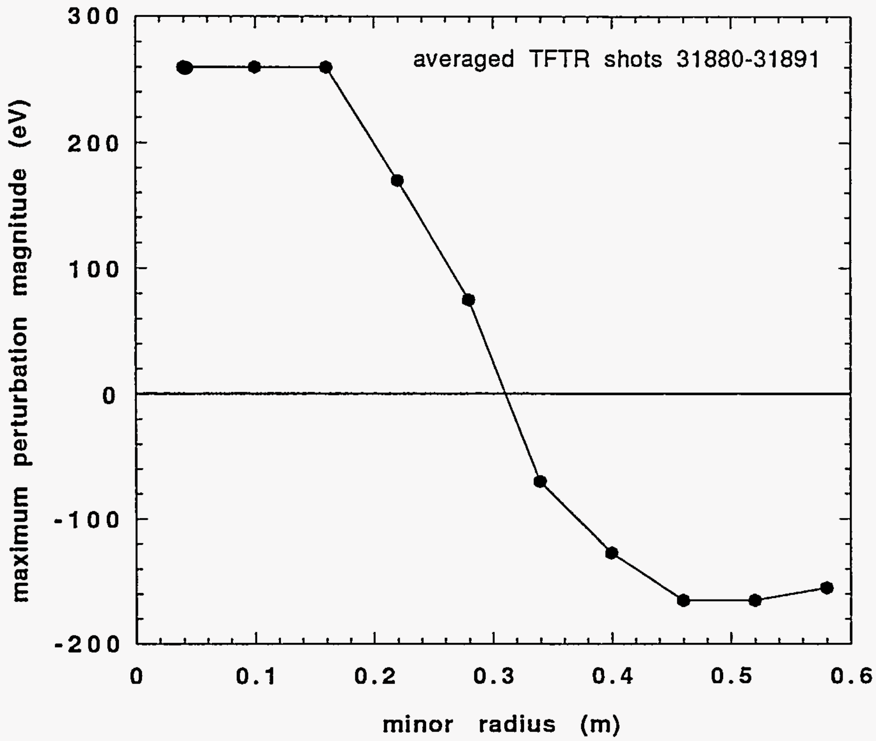

averaged TFTR shots 31880-31891
maximum perturbation magnitude (eV)
300
200
100
0
-100
-200
0
0.1
0.2
0.3
0.4
0.5
0.6
minor radius (m)

FIG. 3

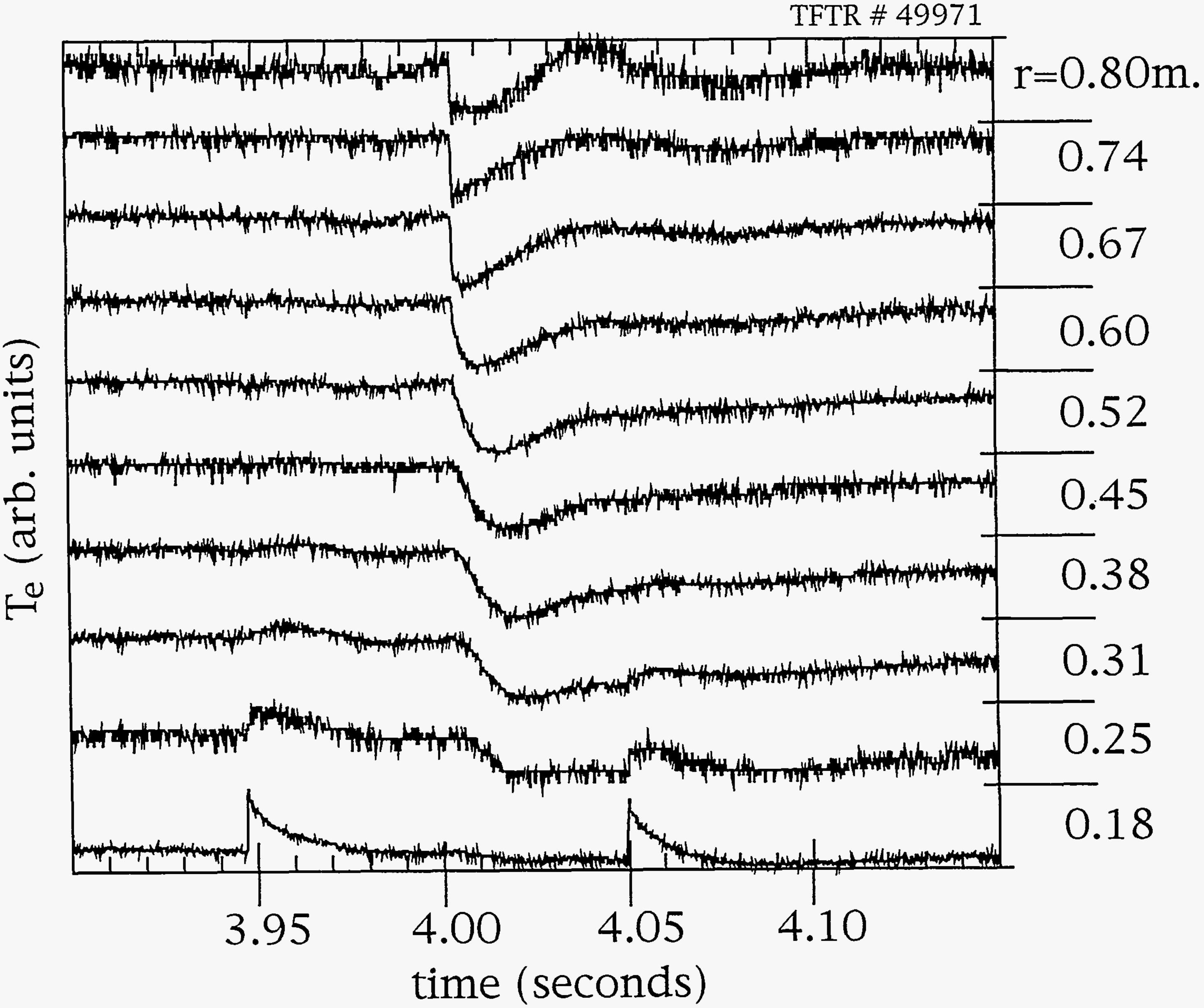
TFTR # 49971
r=0.80m.
0.74
0.67
0.60
0.52
0.45
0.38
0.31
0.25
0.18
$T_e$ (arb. units)
3.95
4.00
4.05
4.10
time (seconds)

FIG. 4a

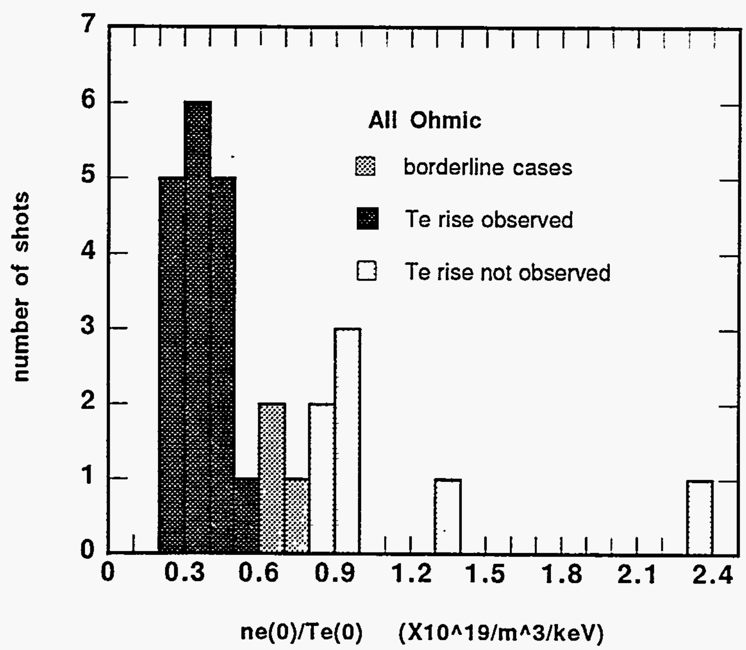
All Ohmic
borderline cases
Te rise observed
Te rise not observed
number of shots
0
1
2
3
4
5
6
7
0
0.3
0.6
0.9
1.2
1.5
1.8
2.1
2.4
ne(0)/Te(0) (X10^19/m^3/keV)

FIG. 4b

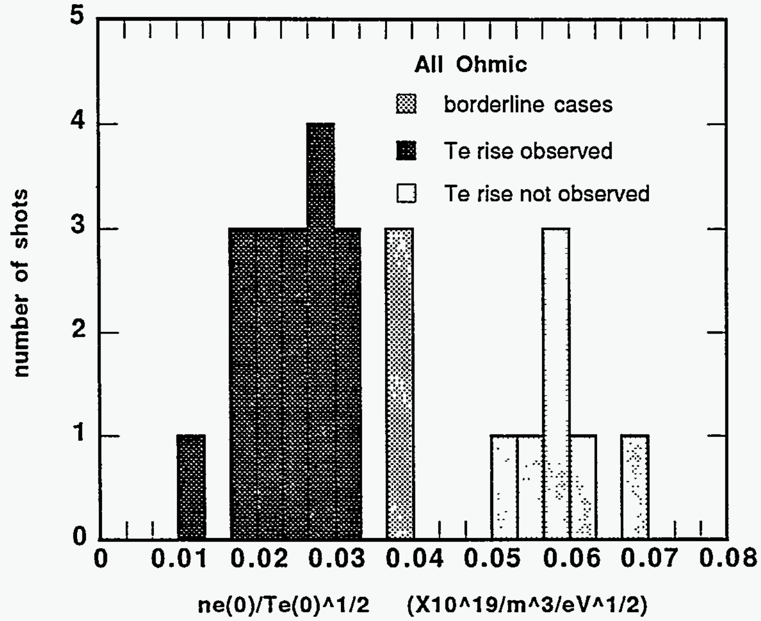

All Ohmic
borderline cases
Te rise observed
Te rise not observed
number of shots
0
1
2
3
4
5
0
0.01
0.02
0.03
0.04
0.05
0.06
0.07
0.08
ne(0)/Te(0)^1/2 (X10^19/m^3/eV^1/2)

FIG. 4c

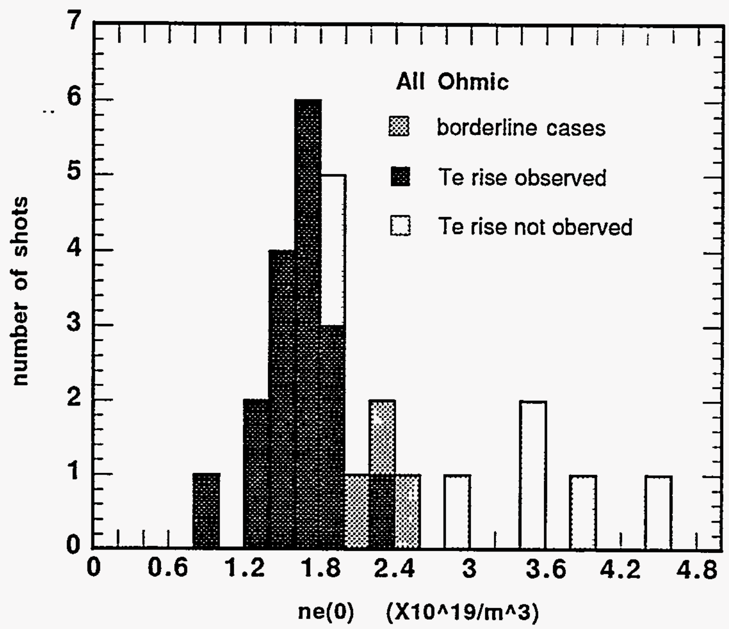

All Ohmic
borderline cases
Te rise observed
Te rise not oberved
number of shots
0
1
2
3
4
5
6
7
0
0.6
1.2
1.8
2.4
3
3.6
4.2
4.8
ne(0) (X10^19/m^3)

FIG. 5

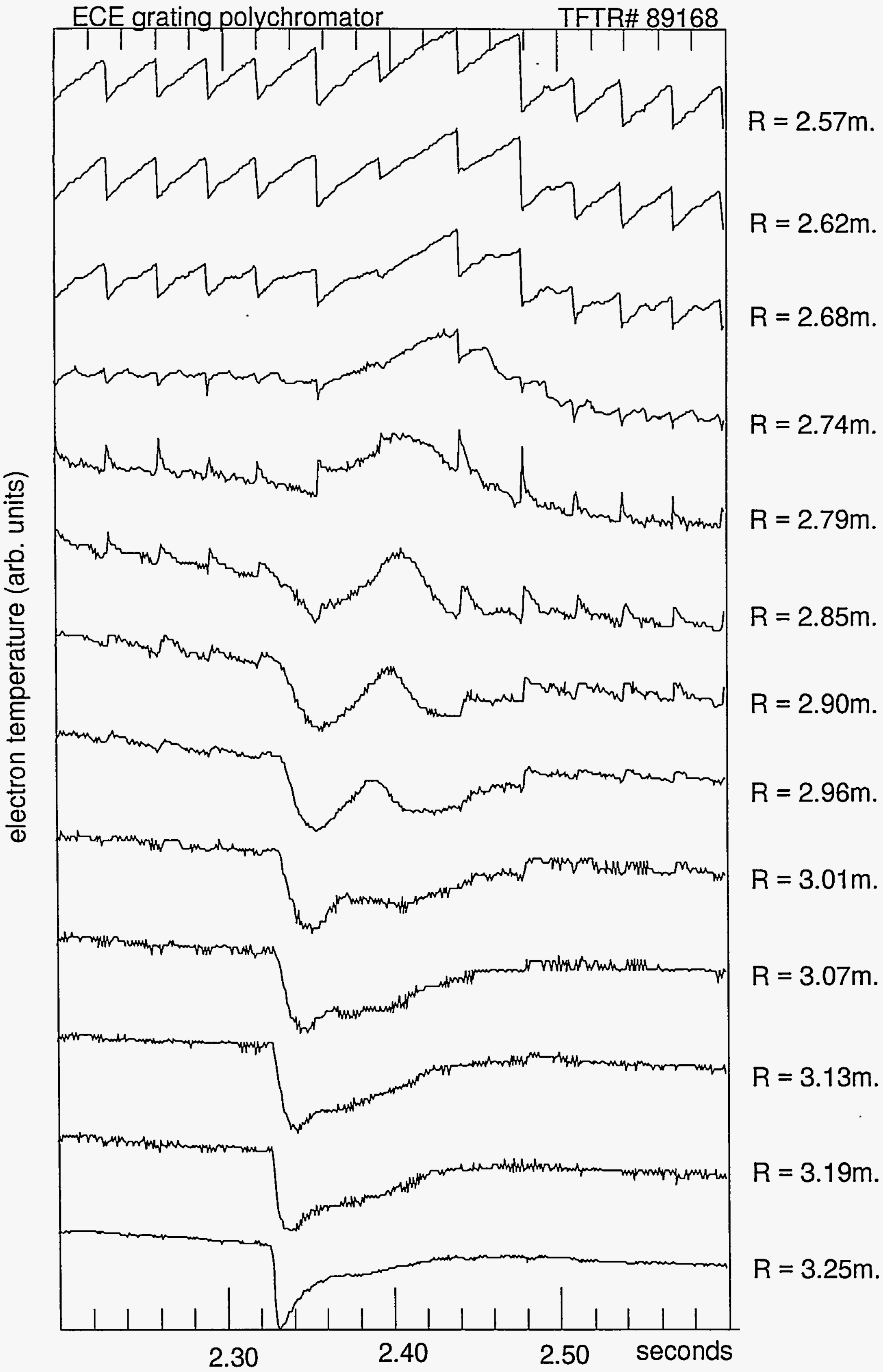
ECE grating polychromator
TFTR# 89168
electron temperature (arb. units)
R = 2.57m.
R = 2.62m.
R = 2.68m.
R = 2.74m.
R = 2.79m.
R = 2.85m.
R = 2.90m.
R = 2.96m.
R = 3.01m.
R = 3.07m.
R = 3.13m.
R = 3.19m.
R = 3.25m.
2.30
2.40
2.50
seconds

FIG. 6

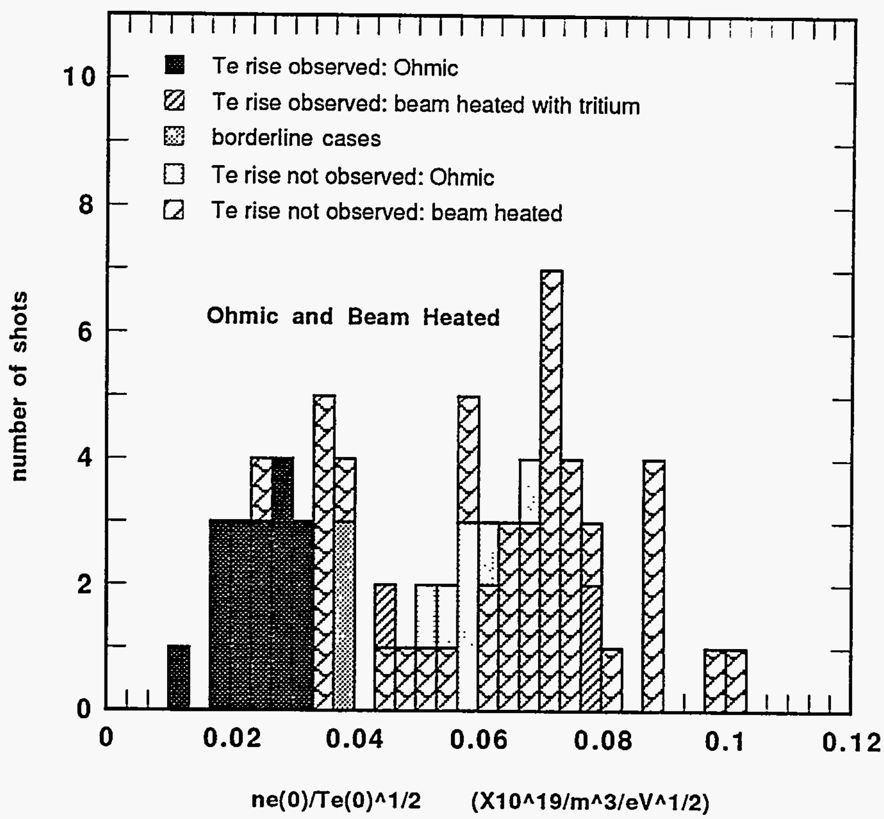

Te rise observed: Ohmic
Te rise observed: beam heated with tritium
borderline cases
Te rise not observed: Ohmic
Te rise not observed: beam heated
Ohmic and Beam Heated
number of shots
0
2
4
6
8
10
0
0.02
0.04
0.06
0.08
0.1
0.12
ne(0)/Te(0)^1/2 (X10^19/m^3/eV^1/2)

FIG. 7

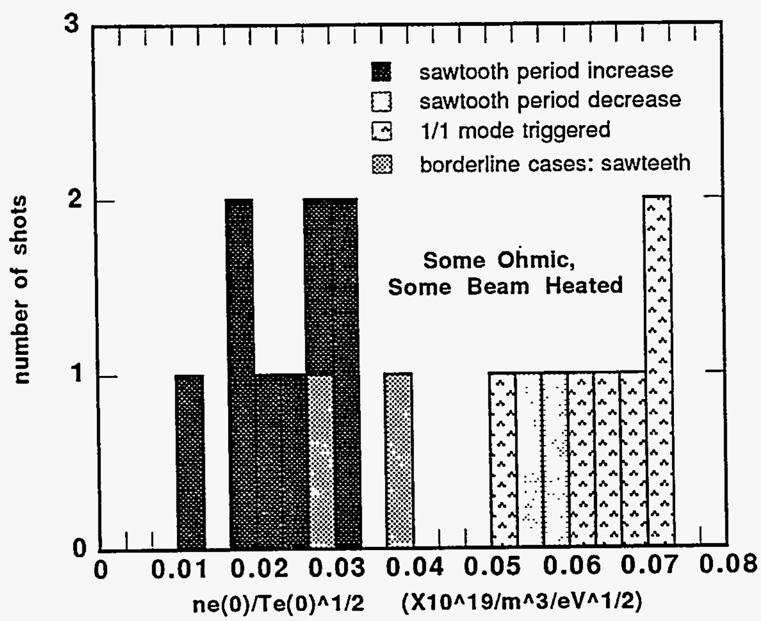

sawtooth period increase
sawtooth period decrease
1/1 mode triggered
borderline cases: sawteeth
Some Ohmic,
Some Beam Heated
number of shots
0
1
2
3
0
0.01
0.02
0.03
0.04
0.05
0.06
0.07
0.08
ne(0)/Te(0)^1/2 (X10^19/m^3/eV^1/2)

FIG. 8

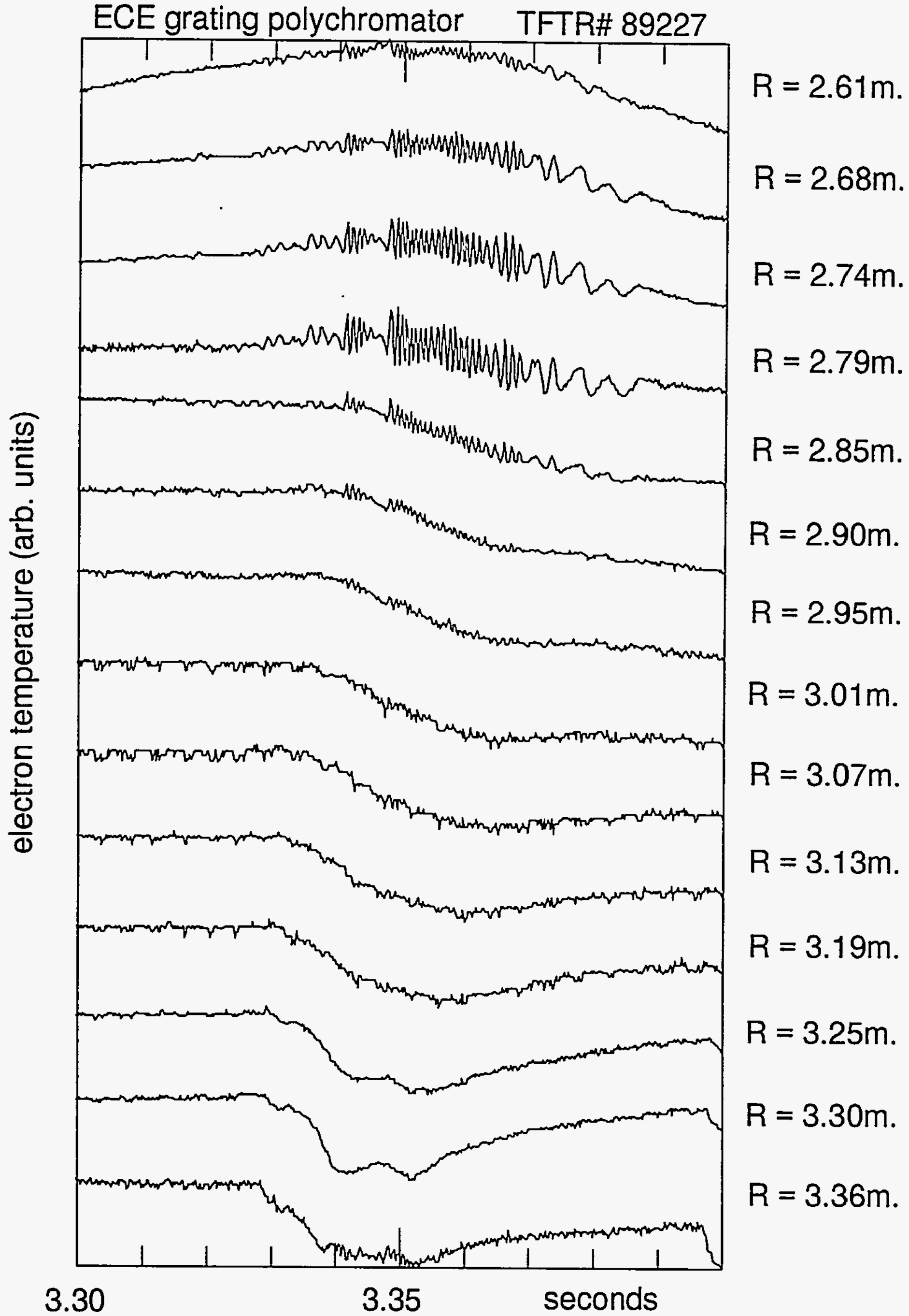

ECE grating polychromator
TFTR# 89227
R = 2.61m.
R = 2.68m.
R = 2.74m.
R = 2.79m.
R = 2.85m.
R = 2.90m.
R = 2.95m.
R = 3.01m.
R = 3.07m.
R = 3.13m.
R = 3.19m.
R = 3.25m.
R = 3.30m.
R = 3.36m.
electron temperature (arb. units)
3.30
3.35
seconds

FIG. 9

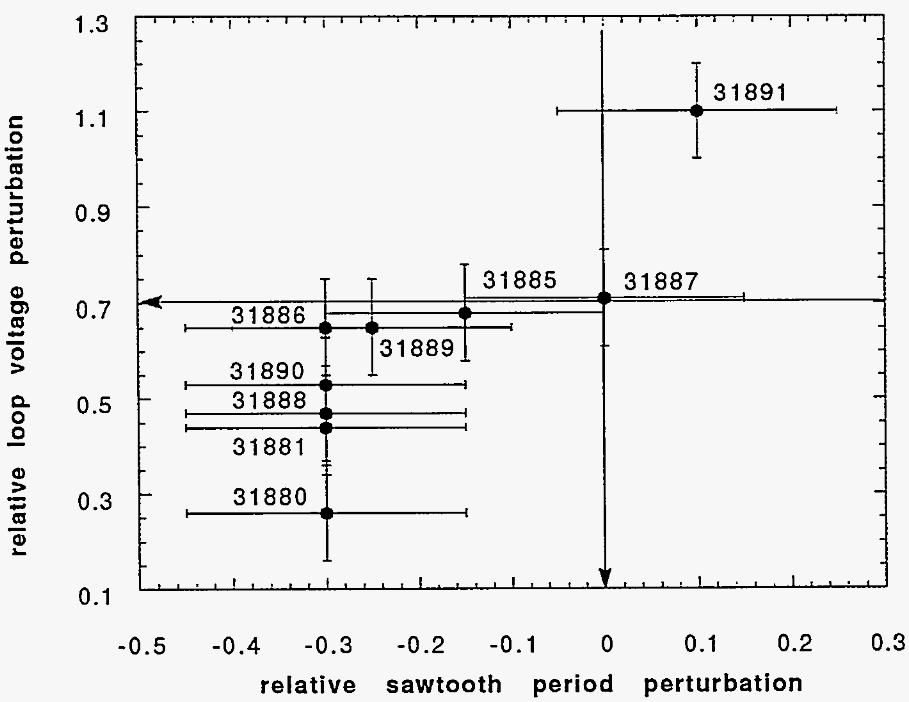

1.3
1.1
0.9
0.7
0.5
0.3
0.1
relative loop voltage perturbation
-0.5
-0.4
-0.3
-0.2
-0.1
0
0.1
0.2
0.3
relative sawtooth period perturbation
31891
31885
31887
31886
31889
31890
31888
31881
31880

FIG. 10

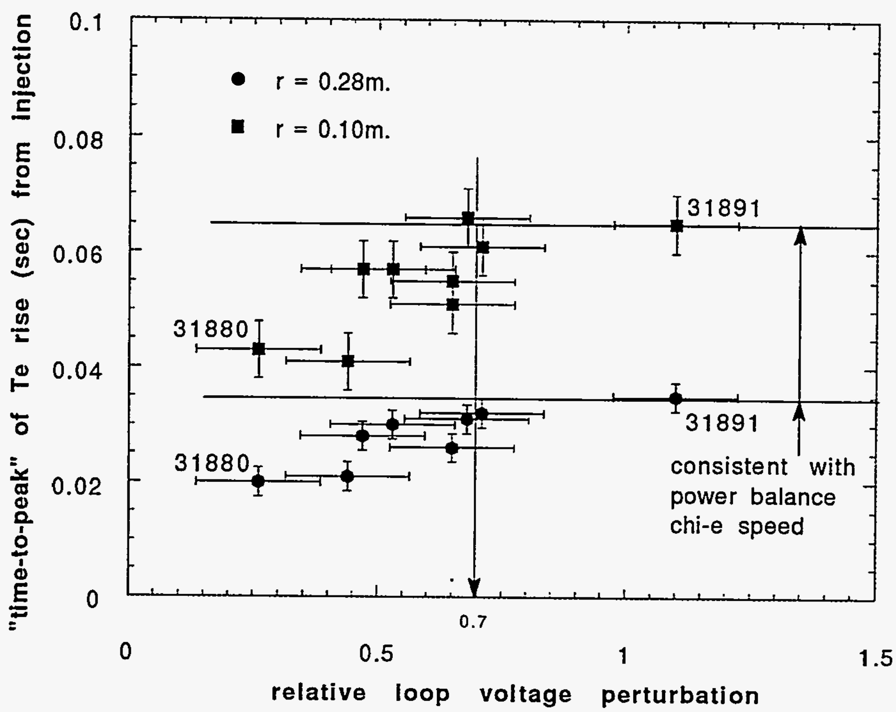

"time-to-peak" of Te rise (sec) from injection
0.1
0.08
0.06
0.04
0.02
0
r = 0.28m.
r = 0.10m.
31891
31880
31891
31880
consistent with
power balance
chi-e speed
0.7
0
0.5
1
1.5
relative loop voltage perturbation

FIG. 11

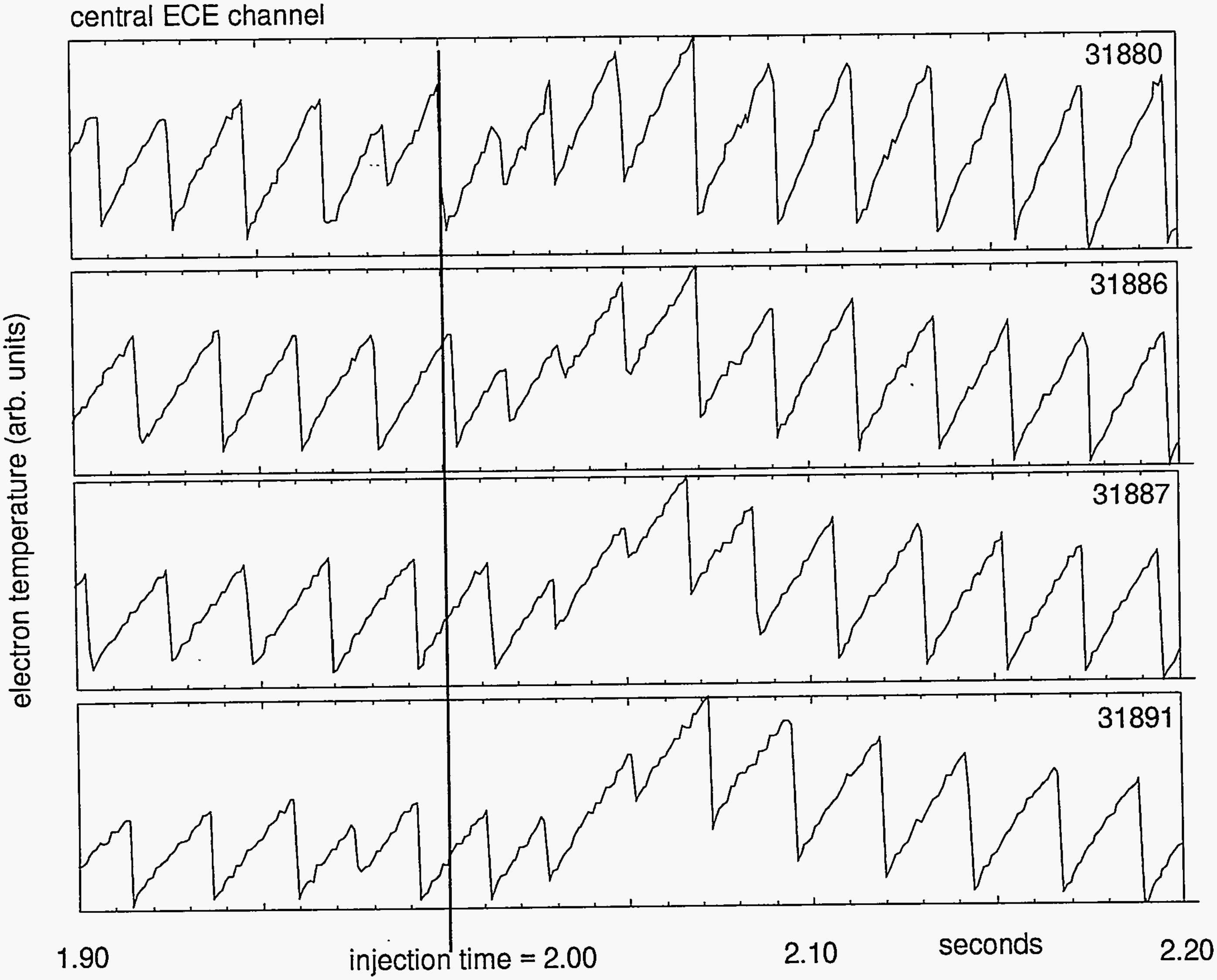

central ECE channel
31880
31886
31887
31891
electron temperature (arb. units)
1.90
injection time = 2.00
2.10
seconds
2.20

FIG. 12

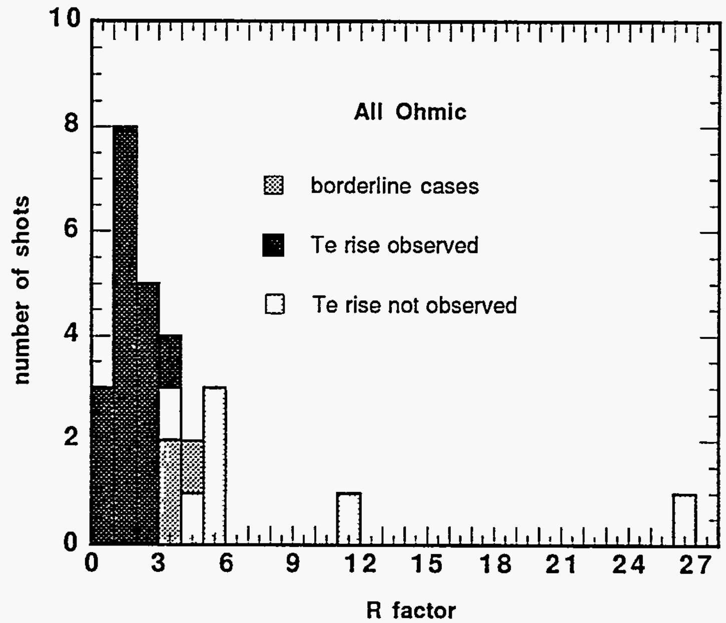

All Ohmic
borderline cases
Te rise observed
Te rise not observed
number of shots
R factor
0
2
4
6
8
10
0
3
6
9
12
15
18
21
24
27